Estimation of Large-scale Wind Field Characteristics using Supervisory Control and Data

Preprint

Michael Sinner,[1] Lucy Y. Pao,[2] and Jennifer King[2]

1 University of Colorado Boulder
2 National Renewable Energy Laboratory

Presented at the American Control Conference (ACC)
July 1–3, 2020

NREL is a national laboratory of the U.S. Department of Energy
Office of Energy Efficiency & Renewable Energy
Operated by the Alliance for Sustainable Energy, LLC

This report is available at no cost from the National Renewable Energy Laboratory (NREL) at www.nrel.gov/publications.

Contract No. DE-AC36-08GO28308

Conference Paper
NREL/CP-5000-76003
August 2020

Estimation of Large-scale Wind Field Characteristics using Supervisory Control and Data

Preprint

Michael Sinner,[1] Lucy Y. Pao,[2] and Jennifer King[2]

1 University of Colorado Boulder
2 National Renewable Energy Laboratory

Suggested Citation
Sinner, Michael, Lucy Y. Pao, and Jennifer King. 2020. *Estimation of Large-scale Wind Field Characteristics using Supervisory Control and Data: Preprint*. Golden, CO: National Renewable Energy Laboratory. NREL/CP-5000-76003.
https://www.nrel.gov/docs/fy20osti/76003.pdf.

Contract No. DE-AC36-08GO28308

Conference Paper
NREL/CP-5000-76003
August 2020

National Renewable Energy Laboratory
15013 Denver West Parkway
Golden, CO 80401
303-275-3000 • www.nrel.gov

NOTICE

This work was authored [in part] by the National Renewable Energy Laboratory, operated by Alliance for Sustainable Energy, LLC, for the U.S. Department of Energy (DOE) under Contract No. DE-AC36-08GO28308. Funding provided by the U.S. Department of Energy Office of Energy Efficiency and Renewable Energy Wind Energy Technologies Office. The views expressed herein do not necessarily represent the views of the DOE or the U.S. Government. The U.S. Government retains and the publisher, by accepting the article for publication, acknowledges that the U.S. Government retains a nonexclusive, paid-up, irrevocable, worldwide license to publish or reproduce the published form of this work, or allow others to do so, for U.S. Government purposes.

Cover Photos by Dennis Schroeder: (clockwise, left to right) NREL 51934, NREL 45897, NREL 42160, NREL 45891, NREL 48097, NREL 46526.

NREL prints on paper that contains recycled content.

Estimation of Large-scale Wind Field Characteristics using Supervisory Control and Data Acquisition Measurements

Michael Sinner[1,2], Lucy Y. Pao[1], and Jennifer King[2]

***Abstract*— As the wind energy industry continues to push for increased power production and lower cost of energy, the focus of research has expanded from individual turbines to entire wind farms. Among a host of interesting problems to be solved when considering the wind farm as a whole, we consider the challenge of scalar field e stimation, b ased o n information already collected at the individual turbine level. We aim to estimate the large-scale, low-frequency characteristics of the wind field, s uch a s t he m ean w ind d irection a nd t he overall decrease in wind speed across the farm, and employ a Kalman filter t hat m odels t he w ind fi eld us ing a po lynomial function. We compare the proposed method's performance to both a simple averaging technique and filtering o f i ndividual turbine measurements. The method presented is not limited to wind turbines and is applicable in other situations where multiple remote agents are used to estimate a scalar field.**

I. INTRODUCTION

Wind energy now plays an important role in the energy market with 591 GW of installed capacity worldwide, 14% market penetration in the European Union, and 6.5% market penetration in the United States [1]. In recent years, researchers have begun to look at the wind farm as a whole, as opposed to considering individual turbine behavior and power production. This shift has led to the idea of treating the wind farm as a 'wind plant' and produced a host of wind farm/plant-related control problems, including optimal power production [2]–[7] and load mitigation [2], [3], [5]; power reference tracking (active power control) [8]–[11]; and communication and consensus [11]–[16].

This work focuses on the latter of these problems. Various elements of the turbine control system, most notably the yaw controller, rely on measurements of the local wind conditions at the turbine, such as the wind speed and wind direction. These measurements are usually taken on the turbine nacelle, behind the rotor in the turbulent wake region, but are taken to be representative of the wind condition directly in front of the turbine rotor. To the authors' knowledge, the standard method is to apply simple filtering to the measured signals and make no use of external information in producing a better-informed estimate of the local wind condition.

Several approaches addressing this issue are presented in Annoni et al. [14]. The main approach used is a wind direction consensus solved by distributed optimization, which is shown to perform well compared to averaging techniques [14]. Although the distributed algorithm used allows the problem to be solved quickly enough for real-time implementation, the method still relies on solving an optimization problem online (iteratively), which could be prohibitive in applications where high-rate communication is infeasible. Further, the consensus and averaging approaches presented do not take into account the time dependency of the wind, essentially assuming a new wind condition at every time step.

In contrast, the Kalman filtering method we present here has the benefits of being computationally simple, including a dynamic model of the wind field, and having well-defined probabilistic properties, albeit limited to the nominal case. Wind field modeling for the purpose of estimation has been approached using various techniques [17]–[19]. Our approach is to consider only the lowest-frequency characteristics: the mean wind speed and direction. We do not aim to provide resolution to the level of individual turbine wakes [17]–[19], time-varying turbulent structures [17], or complex terrain, although we suggest an approach for addressing the latter in Sec. VI-C. However, our method could be used to provide insight into the overall losses in wind speed resulting from waking of turbines [20], and how these losses are distributed through the farm, based on data that are already gathered at the turbines.

This paper is organized as follows. Sec. II describes the wind field model. Sec. III presents the Kalman filtering method used in this work. Sec. IV verifies the approach on a nominal case, and Sec. V applies our method to data gathered from a large wind farm. Extensions and conclusions are discussed in Secs. VI & VII, respectively.

A. Motivations

The main motivation behind this work is to provide more accurate estimates of the wind field at the turbines than can be generated using the locally gathered wind speed and wind direction measurements alone, without adding extra sensors. These estimates can then be used to improve the performance of individual turbines as well as of larger-scale wind plants. Further, the proposed method can be used to estimate values

[1] Department of Electrical, Computer, and Energy Engineering, University of Colorado, Boulder, CO 80309, USA. michael.sinner@colorado.edu, pao@colorado.edu.

[2] National Renewable Energy Laboratory, Golden, CO 80401, USA. michael.sinner@nrel.gov, jennifer.king@nrel.gov.

at locations where measured data are unavailable, such as turbines with faulty sensors or coordinates where a turbine does not exist (see Sec. VI-A).

B. Notation

We let $x \in \mathbb{R}^{n_x}$ and $y \in \mathbb{R}^{n_y}$ be the state and (noise-corrupted) output of a generic dynamical system and use $(X_i, Y_i) \in \mathbb{R}^2$ to refer to the Cartesian coordinates of point i. We denote by $\hat{y}$ and y^{t} an estimated output and 'true' (noiseless) output, respectively. Let $z_i \in \mathbb{R}^{n_x}$ be the vector of regressors for point i, which is the generalized input to a polynomial of degree d with input dimension m. By 'generalized input,' we mean that if we are considering a second-order polynomial ($d = 2$) with two inputs ($m = 2$)

$$f(X_i, Y_i) = p_{X^2} X_i^2 + p_{Y^2} Y_i^2 + p_{XY} X_i Y_i + p_X X_i + p_Y Y_i + p_0,$$

where the p are the polynomial coefficients, then

$$z_i = \begin{bmatrix} X_i^2 & Y_i^2 & X_i Y_i & X_i & Y_i & 1 \end{bmatrix}^\top$$

and

$$x = \begin{bmatrix} p_{X^2} & p_{Y^2} & p_{XY} & p_X & p_Y & p_0 \end{bmatrix}^\top$$

so that we can equivalently write $f(z_i) = x^\top z_i$. In general, for a polynomial, $n_x = (d+m)!/(d!m!)$.

Further notation will be introduced as it appears.

II. WIND FIELD MODEL

Although various models have been suggested for wind field estimation [17]–[19], the approach we take considers only a very coarse wind field model.

A. Static Field Model

The basic notion that we follow is that of linear regression, using a least-squares approach: given a set of (noisy) data points, we would like to find the function $f \in \mathcal{F}$ that minimizes the ℓ^2 norm of the residual between the function and the data. The function space $\mathcal{F}$ (which should be linear in its parameters) is specified beforehand; for this work, we consider the space of polynomials of degree d with input dimension m. Because we are modeling a scalar field over physical space, we use $m = 2$ to define a two-dimensional wind farm, although the method we present can be easily extended to a three-dimensional case.

The polynomial is then represented as an inner product

$$f(z) = x^\top z \tag{1}$$

where z is the regressor vector and x is the vector of polynomial coefficients (see Sec. I-B).

The (static) least-squares regression problem for polynomials is then

$$\underset{x}{\text{minimize}} \sum_{i=1}^{N} \varepsilon_i^2 \tag{2a}$$

$$\text{subject to } \varepsilon_i = x^\top z_i - y_i \tag{2b}$$

where $\{(z_i, y_i)\}_{i=1,\ldots,N}$ are the problem data.

B. Dynamic Field Model

Since the large-scale wind characteristics (speed, direction) change over time, the solution to problem (2) degrades over time. While (2) could be solved repeatedly, this approach does not account for the wind field dynamics. As such, we propose a simple discrete-time model for the dynamic behavior of the wind field

$$x(k+1) = x(k) + w(k) \tag{3}$$

where $w(k) \sim \mathcal{N}(0, Q)$ is process noise that causes the wind field to vary with time in a stochastic way. The dynamics (3) represent a random walk with Gaussian steps in n_x dimensions, and model variations in the wind field by allowing the field at time $k+1$ to be slightly different from that at time k.

C. Measurement Model

A single point in the scalar field defined by f is found as $f(z) = x^\top z = z^\top x$. Stacking outputs from N different inputs z_i, we have

$$y^{\mathrm{t}} \stackrel{\text{def}}{=} \begin{bmatrix} f(z_1) \\ \vdots \\ f(z_N) \end{bmatrix} = \begin{bmatrix} z_1^\top \\ \vdots \\ z_N^\top \end{bmatrix} x = Cx \tag{4}$$

where $C \stackrel{\text{def}}{=} \begin{bmatrix} z_1 & \cdots & z_N \end{bmatrix}^\top$. Using the example given in Sec. I-B (quadratic polynomial, two inputs), we would have

$$C = \begin{bmatrix} X_1^2 & Y_1^2 & X_1 Y_1 & X_1 & Y_1 & 1 \\ \vdots & \vdots & \vdots & \vdots & \vdots & \vdots \\ X_N^2 & Y_N^2 & X_N Y_N & X_N & Y_N & 1 \end{bmatrix}$$

for a set of N measurement points $\{(X_i, Y_i)\}_{i=1,\ldots,N}$.

D. Standard State-Space Form

By adding measurement noise $v(k) \sim \mathcal{N}(0, R)$ to the true output (4) and combining with the dynamic model (3), we have the standard (uncontrolled) state-space form

$$x(k+1) = Ax(k) + w(k) \tag{5a}$$

$$y(k) = Cx(k) + v(k) \tag{5b}$$

where the system matrix $A = I_{n_x}$, the $n_x \times n_x$ identity matrix, and the output matrix $C \in \mathbb{R}^{n_y \times n_x}$ is constructed by stacking the generalized inputs z_i at the points $i = 1, \ldots, N$.

III. KALMAN FILTER APPROACH

The steady-state Kalman filtering method [21] is applied to the system model (5) to produce estimates $\hat{x}(k)$ and $\hat{y}(k)$ given a history of noisy observations $y(k), y(k-1), ..., y(0)$. For the Kalman filter to be realized, we assume that (A, C) is observable. Because $A = I_{n_x}$, the observability condition reduces to a requirement that C has rank n_x, which is the same condition needed for uniqueness of the solution to the static least-squares problem (2).

The steady-state state and output estimates are

$$\hat{x}(k+1) = A\left(\hat{x}(k) + L\left(y(k) - C\hat{x}(k)\right)\right) \tag{6a}$$

$$\hat{y}(k) = C\hat{x}(k) \tag{6b}$$

where $L = PC^\top \left(CPC^\top + R\right)^{-1}$ is the steady-state Kalman gain and P is the positive definite solution to the discrete algebraic Riccati equation (DARE)

$$P = APA^\top + Q - APC^\top \left(CPC^\top + R\right)^{-1} CPA^\top . \quad (7)$$

The gain L is optimal in that it minimizes the trace of the posterior state error covariance

$$P^+(k) \stackrel{\text{def}}{=} \mathsf{E}\left[\left(x(k) - \hat{x}^+(k)\right)\left(x(k) - \hat{x}^+(k)\right)^\top\right]$$

as $k \to \infty$ (steady state), where $\hat{x}^+(k) = \hat{x}(k) + L\left(y(k) - C\hat{x}(k)\right)$ is the posterior state estimate at time k.

A. Implicit Assumptions and Validity

Using the state-space model (5) to represent the wind field, we can proceed to apply the Kalman filter directly under two important assumptions:

1) (A, C) is an accurate model of the wind field.
2) The process noise $w(k)$ and measurement noise $v(k)$ are additive white Gaussian noise sequences with covariances Q and R, respectively.

Under these assumptions, many properties and guarantees of performance of the Kalman filter can be derived [21]. Our application, however, is unlikely to strictly meet them. In particular, modeling a turbulent wind field using a low-order polynomial can only hope to capture large, low-frequency variations, and small, high-frequency turbulent structures will not be captured. On the other hand, Kalman filters are popular in the literature across various fields where the assumptions made cannot be shown to strictly hold, and even without technical guarantees they can perform well in many applications. We also demonstrate this to be the case.

B. Theory on Output Covariance

The Kalman filter, under assumptions 1) and 2), has well-known properties regarding the statistics of the estimate. Of interest are the properties of the output estimate $\hat{y}(k)$. In particular, it can be shown that as $k \to \infty$, the output estimation error $e_y(k) = y^{\mathrm{t}}(k) - \hat{y}(k)$ is distributed as $e_y(k) \sim \mathcal{N}(0, CPC^\top)$. This allows us to quantify the error in our estimate of the field characteristics, although we again stress that this result holds only when the assumptions are valid.

IV. VERIFICATION TESTING

We verify the proposed algorithm using a simulated wind farm with $N = 16$ turbines in an evenly-spaced 4-by-4 grid with 800 m spacing. We consider a wind field with speed and direction components in a two-dimensional ($m = 2$) farm, and choose a linear fit ($d = 1$) for each scalar field for ease of illustrating the method (higher-order polynomials could be used to improve the model fit and capture more local effects). Thus, $z_i = \begin{bmatrix} X_i & Y_i & 1 \end{bmatrix}^\top$. Because we are producing estimates for both speed U and direction θ, there are two outputs for every point in the field, so $n_y = 2N = 32$ and

$$C = \begin{bmatrix} C_{\text{speed}} & 0 \\ 0 & C_{\text{direction}} \end{bmatrix} \in \mathbb{R}^{32\times 6}$$

where, in this case,

$$C_{\text{speed}} = C_{\text{direction}} = \begin{bmatrix} 0 & 0 & 1 \\ 800 & 0 & 1 \\ \vdots & \vdots & \vdots \\ 2400 & 2400 & 1 \end{bmatrix} .$$

The simulated wind field is generated by setting an initial value $x(0) = \begin{bmatrix} 0 & 0 & 5 & 0 & 0 & -\pi/2 \end{bmatrix}^\top$ (uniform 5 m/s winds from the west) and propagating x according to (3) by drawing the $w(k)$ from $\mathcal{N}(0, Q)$ with

$$Q = \begin{bmatrix} Q_{\text{speed}} & 0 \\ 0 & Q_{\text{direction}} \end{bmatrix}$$

where $Q_{\text{speed}} = \operatorname{diag}\left(\begin{bmatrix} 2\times 10^{-9} & 2\times 10^{-9} & 2\times 10^{-3} \end{bmatrix}\right)$ relates to wind speed magnitude (in m/s) and $Q_{\text{direction}} = \operatorname{diag}\left(\begin{bmatrix} 1\times 10^{-9} & 1\times 10^{-9} & 1\times 10^{-3} \end{bmatrix}\right)$ to wind direction (in radians). Turbine measurements are generated using (5b) with $v(k)$ sampled from $\mathcal{N}(0, R)$ with $R = I_{32}$.

Q and R have not been carefully tuned for this illustrative study. In a practical application, we suggest that the user set $R = I_N$ (assuming that the sensor properties at each turbine are the same), and then manually tune the entries of Q to achieve good performance for a set of test data. The user should also experiment with the polynomial order d.

By our formulation, the models involved with speed measurement/estimation and direction measurement/estimation are completely decoupled scalar fields and could just as easily be run using two separate Kalman filters; however, this need not be the case (especially if there is known correlation between different sensors). If a coupled estimator is used, more care will be required to select appropriate covariances Q and R.

Once 'truth' data have been generated, we apply the Kalman filtering approach to generate estimates of the wind speed and direction at each turbine (initializing with $\hat{x}(0) = 0$). For the wind direction estimates, we apply the heuristic that the innovation $y(k) - C\hat{x}(k)$ should be wrapped to the interval $(-\pi, \pi]$ [22].

Results from verification testing have been omitted for brevity, but we confirm that the Kalman filter is operating as designed, and proceed to present results testing our method on field data.

V. TESTING ON FIELD DATA

For realistic testing, we apply our method to supervisory control and data acquisition (SCADA) data collected at a functioning wind farm, where the assumptions in Sec. III-A are unlikely to hold. The Kalman filter implementation is the same as that described in Sec. IV, with the dimension of the measurement noise covariance matrix scaled up appropriately. We use the following alternative approaches for comparison to the Kalman filter approach of Secs. III & IV.

A. Simple Mean

Perhaps the simplest 'consensus' approach to produce an estimate of the wind field at point i is to simply take the average over all N measurement points at the previous time [14], i.e.,

$$\hat{y}_i(k+1) = \frac{1}{N}\sum_{j=1}^{N} y_j(k)\,. \tag{8}$$

The spatial mean (8) takes account of neither time evolution nor spatial variations of the field.

The simple mean is a limiting case of the Kalman filter estimate as Q becomes large and $d = 0$ (constant polynomial function). Assuming that all point measurements are equally noisy (and uncorrelated), then $R = rI_N$. Because $d = 0$, $n_x = 1$ regardless of m. This means that $Q = q, P = p \in \mathbb{R}_{\geq 0}$, $A = 1$, and $C = \mathbb{1}_N$ (the N-dimensional vector of 1s). x represents the spatially constant quantity of interest (mean wind speed or direction).

The DARE (7) then reduces to $p^2 - qp - {}^{qr}/_{N} = 0$ with positive-definite solution

$$p = \frac{q}{2} + \frac{\sqrt{q^2 + \frac{4r}{N}q}}{2} \tag{9}$$

and the estimates (6) become

$$\hat{x}(k+1) = \frac{r}{r+Np}\hat{x}(k) + \frac{p}{r+Np}\sum_{j=1}^{n} y_i(k) \tag{10a}$$

$$\hat{y}(k) = \mathbb{1}_N \hat{x}(k)\,. \tag{10b}$$

As $q \to \infty$ while r stays fixed, $p \to q \to \infty$ from (9), and

$$\lim_{p\to\infty} \hat{y}(k+1) = \mathbb{1}_N \frac{1}{N}\sum_{j=1}^{N} y_j(k)\,.$$

B. Individual Measurement Filtering

To our knowledge, a common technique used in industry for smoothing measured data obtained at a turbine is to filter the measured signal to remove both measurement noise and higher-frequency turbulent effects. We therefore use a single-input single-output (SISO) Kalman filter (6).

In the SISO case ($y(k), \hat{y}(k) \in \mathbb{R}$), the state is observable only for $d = 0$, because no information about the spatial gradient (or higher derivatives) can be provided from a single point measurement. We therefore use $\hat{x} \in \mathbb{R}$, and let $Q_{\text{speed}} = 2 \times 10^{-3}$, $Q_{\text{direction}} = 1 \times 10^{-3}$, and $R_{\text{speed}} = R_{\text{direction}} = 1$. We thus arrive at a first-order filter for both the wind direction and speed at each turbine.

The main drawback of this method is that it cannot remove any local bias from the measurements. Further, under a sensor fault, the turbine likely has to be taken out of operation (see Sec. VI-A). On the other hand, this method requires no communication.

C. Test Scenario

We test the proposed method, as well as the alternatives described in Secs. V-A and V-B, on 1000 minutes of 0.0167 Hz data from an operational wind farm with approximately 200 turbines [14]. All simulations are initialized with $\hat{x}(0) = 0$ to represent no prior knowledge of the wind condition. We provide only a subset of normalized results to protect the anonymity of the wind farm operator.

D. Results

The time series results of the test are shown for two turbines in the farm (Figs. 1 and 2) to visually identify features of the different estimates. A faulty direction measurement is apparent in Fig. 1. While the full Kalman filter (full KF) and simple mean are comparable, the individual Kalman filter (SISO KF) does not benefit from measurements from other turbines and is unable to handle a wind direction sensor fault. The SISO KF also has significant delay, but this can likely be improved with different choices of Q and R.

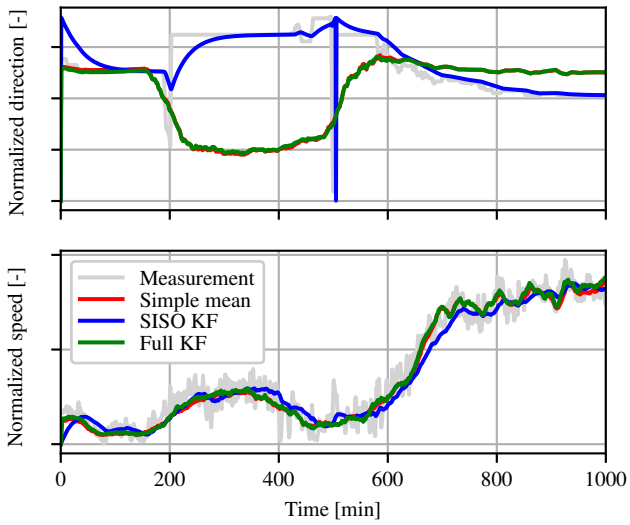

Fig. 1. Estimates for one wind turbine in the farm: raw 1-minute data (measurement), simple mean (Sec. V-A), individual measurement filter (SISO KF, Sec. V-B), and proposed Kalman filter method (full KF, Sec. III).

Sensors appear to be behaving correctly in Fig. 2 and the SISO KF estimate aligns moderately well with the other estimates. However, both the simple mean and full KF are better able to track the wind direction change that occurs around 200 s as a result of other turbines' measurements.

We also include a spatial representation of the estimates in Fig. 3. The figure shows only a subset of the turbines in the farm, but provides some insight into the algorithm behavior. In particular, we can see that the Kalman filter behaves similarly to the simple mean except in the lower-right region, whereas the individual measurement filter shows significant disagreement between some neighboring turbines.

Although 'truth' measurements are difficult to obtain at the turbine location, the estimates can be validated against a met mast near the farm, which (at least in principle) provides an accurate measure of the wind at its location. The Kalman

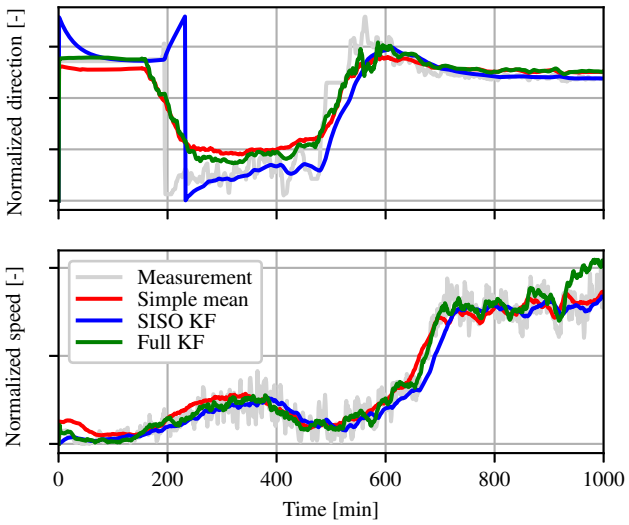

Fig. 2. Estimates for a second turbine in the farm: raw 1-minute data (measurement), simple mean (Sec. V-A), individual measurement filter (SISO KF, Sec. V-B), and proposed Kalman filter method (full KF, Sec. III).

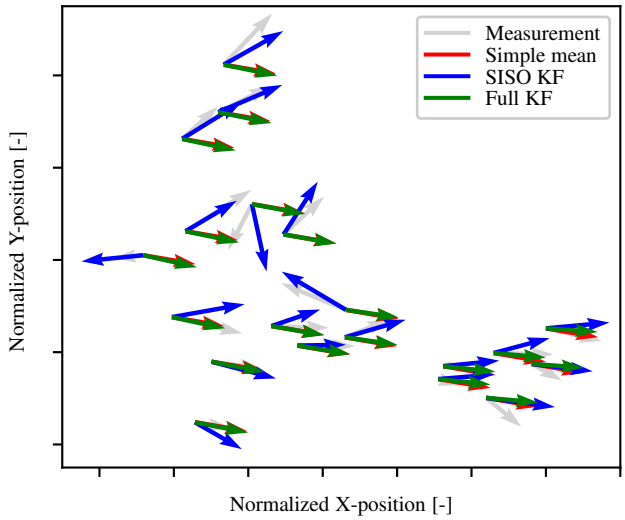

Fig. 3. A subset of the turbines in the farm, chosen randomly, at a single time step. Raw 1-minute data (measurement), simple mean (Sec. V-A), individual measurement filter (SISO KF, Sec. V-B), and proposed Kalman filter method (full KF, Sec. III). Arrow direction indicates the estimated wind direction while arrow length indicates speed. For data protection reasons, the X- and Y-direction unit lengths are not equal.

filter output can be extended to provide an estimate at the met mast location using the method described in Sec. VI-A, while the simple average can also be used as an estimate of the speed at the met mast location. On the other hand, the SISO Kalman filter estimates only the wind speed at the turbine location, and is therefore not compared here. The met mast provides only wind speed data, so only wind speed (and not wind direction) estimates are analyzed.

Fig. 4 (top) displays the met mast wind speed signal as well as the Kalman filter and simple average estimates of the wind speed. Fig. 4 (bottom) displays the error between the met mast data and each of the estimates. The Kalman filter reduces the root-mean-squared wind speed estimation error

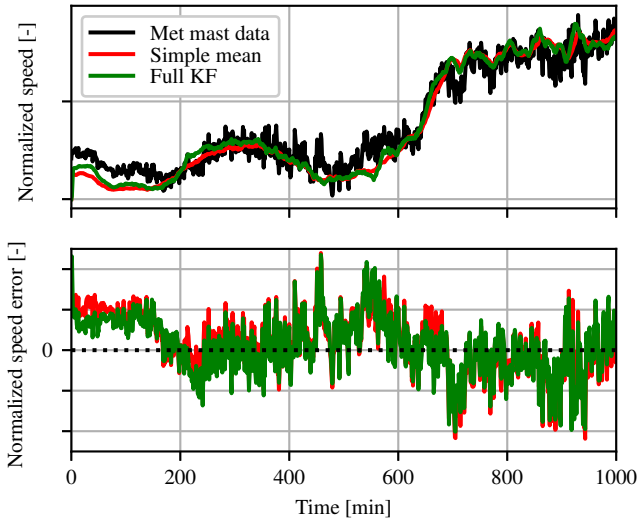

Fig. 4. Wind speed estimates at the met mast location. The top plot shows the met mast wind speed data along with speed estimates from the Kalman filter (full KF) and simple average, whereas the lower plot shows the error between the met mast data and the estimates.

by 4.8% compared to the simple average.

VI. EXTENSIONS

We now describe extensions to the method of Sec. III.

A. Data Interpolation

While we have considered estimating the wind field at the turbine locations, the state x contains information about the wind field everywhere. In particular, a second output matrix C' can be constructed for positions $i' = 1, ..., N'$ such that, using $\hat{y}' = C'\hat{x}$, field values at the i' locations are estimated without measurements at these locations.

This may have several uses, but one important case is when a turbine sensor is faulty—in that case, the faulty turbine can be removed from y and added to y', so that it may continue to operate on the measurements received from other turbines without degrading the estimates at the other turbines. We use this method in Sec. V-D to estimate quantities at a met mast.

B. Time-Varying Wind Characteristics

Global wind properties, such as turbulence intensity, change with time (for example, the atmospheric boundary layer is less turbulent at night than during the day). These variations could be modeled with time-varying noise covariance matrices, i.e., $Q = Q(k)$ and $R = R(k)$. The dynamic Kalman filter [21] can then be implemented in place of the steady-state Kalman filter (6).

C. Breakdown of Farm into Small Pieces

If representing the entire wind field using a single polynomial function is too limiting, the farm can be broken into M spatially linked subsets, as shown in Fig. 5. The mth subset, $m = 1, ..., M$, contains some of the N turbines, i.e., $\mathcal{S}_m \subseteq \{1, ..., N\}$ with cardinality $N_m = |\mathcal{S}_m|$.

The Kalman filter algorithm presented in Sec. III can then be applied to each subset, with (A_m, C_m) replacing (A, C) in

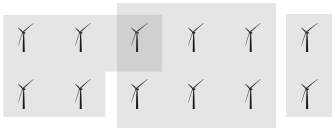

Fig. 5. Example breakdown of a wind farm into $M = 3$ subsets.

the model and with N_m replacing N. Some sort of average is required to handle turbines that lie in the intersection between two or more of the $\mathcal{S}_m$.

D. Distributed Implementation

Computationally, the Kalman filter (6) is straightforward, requiring only relatively small matrix multiplications online, and can therefore be solved quickly on a single computer. In contrast, more sophisticated consensus algorithms that involve solving an optimization problem at each time step can be made tractable by distributing the problem across multiple nodes [14]. However, there may be security and privacy benefits in a distributed approach.

In our model (Sec. II), C contains considerable information about the wind farm layout. Although the layout of a wind farm is perhaps not sensitive information, we imagine that in some applications the type of information stored in C could be sensitive. The centralized approach (6) requires the storage of C at a single location, which creates an easy target for malicious attacks. It could also be desirable to keep the measurements y_i, $i = 1, ..., N$, at the N nodes private.

To handle this, we rewrite (6) as

$$\eta_i(k) = [L]_{:,i}\left(y_i(k) - [C]_{i,:}\hat{x}(k)\right), \quad i = 1, ..., N \tag{11a}$$

$$\hat{x}(k+1) = A\left(\hat{x}(k) + \sum_{i=1}^{N}\eta_i(k)\right) \tag{11b}$$

$$\hat{y}_i(k) = [C]_{i,:}\hat{x}(k), \quad i = 1, ..., N \tag{11c}$$

where $[L]_{:,i}$ denotes the ith column of L and $[C]_{i,:}$ the ith row of C. Now, steps (11a) and (11c) can be carried out locally at the nodes, whereas step (11b) must be computed centrally but does not require explicit knowledge or sharing of C or the y_i. The η_i and $\hat{x}$ must be communicated between the N nodes and the central solver.

VII. CONCLUSIONS AND FUTURE WORK

The Kalman filter appears to perform well in estimating large-scale wind field parameters. Major benefits of this approach include the ability to provide smooth estimates, even in the case of faulty individual turbine sensors, and some predictive behavior for turbines toward the center of the farm, using only measurements already collected at the wind turbines. On the other hand, it is limited by being a parametric model and is unlikely to be able to resolve the wind field down to individual turbine wakes.

A nonparametric, consensus-based optimization approach is presented by Annoni et al. [14]. In comparison to the Kalman filter presented here, Annoni et al.'s method is likely better for resolving around specific terrain features, but involves significantly more computational burden.

REFERENCES

[1] "U.S. wind industry annual market report year ending 2018," American Wind Energy Association, Washington, DC, Tech. Rep., 2019.

[2] P. Fleming, P. M. Gebraad, S. Lee, J.-W. van Wingerden, K. Johnson, M. Churchfield, J. Michalakes, P. Spalart, and P. Moriarty, "Simulation comparison of wake mitigation control strategies for a two-turbine case," *Wind Energy*, vol. 18, no. 12, pp. 2135–2143, 2015.

[3] F. Campagnolo, V. Petrović, C. L. Bottasso, and A. Croce, "Wind tunnel testing of wake control strategies," in *Proc. American Control Conf.*, July 2016, pp. 513–518.

[4] P. Fleming, J. Annoni, J. J. Shah, L. Wang, S. Ananthan, Z. Zhang, K. Hutchings, P. Wang, W. Chen, and L. Chen, "Field test of wake steering at an offshore wind farm," *Wind Energy Science*, vol. 2, no. 1, pp. 229–239, 2017.

[5] E. Bossanyi, "Combining induction control and wake steering for wind farm energy and fatigue loads optimisation," *J. Physics: Conf. Series*, vol. 1037, June 2018.

[6] M. Vali, V. Petrović, S. Boersma, J.-W. van Wingerden, L. Y. Pao, and M. Kühn, "Adjoint-based model predictive control for optimal energy extraction in waked wind farms," *Control Engineering Practice*, vol. 84, pp. 48–62, 2019.

[7] M. F. Howland, S. K. Lele, and J. O. Dabiri, "Wind farm power optimization through wake steering," *Proc. National Academy of Sciences*, vol. 116, no. 29, pp. 14 495–14 500, 2019.

[8] P. Fleming, J. Aho, P. Gebraad, L. Pao, and Y. Zhang, "Computational fluid dynamics simulation study of active power control in wind plants," in *Proc. American Control Conf.*, July 2016, pp. 1413–1420.

[9] J.-W. van Wingerden, L. Pao, J. Aho, and P. Fleming, "Active power control of waked wind farms," *IFAC-PapersOnLine*, vol. 50, no. 1, pp. 4484–4491, 2017, 20th IFAC World Congress.

[10] M. Vali, V. Petrović, S. Boersma, J. van Wingerden, L. Y. Pao, and M. Kühn, "Model predictive active power control of waked wind farms," in *Proc. American Control Conf.*, June 2018, pp. 707–714.

[11] C. J. Bay, J. Annoni, T. Taylor, L. Pao, and K. Johnson, "Active power control for wind farms using distributed model predictive control and nearest neighbor communication," in *Proc. American Control Conf.*, June 2018, pp. 682–687.

[12] S. Baros and M. D. Ilić, "Distributed torque control of deloaded wind DFIGs for wind farm power output regulation," *IEEE Transactions on Power Systems*, vol. 32, no. 6, pp. 4590–4599, Nov. 2017.

[13] N. Gionfra, G. Sandou, H. Siguerdidjane, D. Faille, and P. Loevenbruck, "A distributed consensus control under disturbances for wind farm power maximization," in *Proc. Conf. Decision and Control*, Dec. 2017, pp. 2015–2020.

[14] J. Annoni, C. Bay, K. Johnson, E. Dall'Anese, E. Quon, T. Kemper, and P. Fleming, "Wind direction estimation using SCADA data with consensus-based optimization," *Wind Energy Science*, vol. 4, no. 2, pp. 355–368, 2019.

[15] J. Annoni, E. Dall'Anese, M. Hong, and C. Bay, "Efficient distributed optimization of wind farms using proximal primal dual algorithms," in *Proc. American Control Conf.*, July 2019, pp. 4173–4178.

[16] J. Annoni, C. Bay, P. Fleming, and K. Johnson, "Short-term forecasting across a network for the autonomous wind farm," in *Proc. American Control Conf.*, July 2019, pp. 2837–2842.

[17] G. V. Iungo, C. Santoni-Ortiz, M. Abkar, F. Porté-Agel, M. A. Rotea, and S. Leonardi, "Data-driven reduced order model for prediction of wind turbine wakes," *J. Physics: Conf. Series*, vol. 625, June 2015.

[18] P. M. O. Gebraad, P. A. Fleming, and J. W. van Wingerden, "Wind turbine wake estimation and control using FLORIDyn, a control-oriented dynamic wind plant model," in *Proc. American Control Conf.*, July 2015, pp. 1702–1708.

[19] B. M. Doekemeijer, S. Boersma, L. Y. Pao, T. Knudsen, and J.-W. van Wingerden, "Online model calibration for a simplified LES model in pursuit of real-time closed-loop wind farm control," *Wind Energy Science*, vol. 3, no. 2, pp. 749–765, 2018.

[20] J. Annoni, P. Fleming, A. Scholbrock, J. Roadman, S. Dana, C. Adcock, F. Porté-Agel, S. Raach, F. Haizmann, and D. Schlipf, "Analysis of control-oriented wake modeling tools using lidar field results," *Wind Energy Science*, vol. 3, no. 2, pp. 819–831, 2018.

[21] D. Simon, *Optimal state estimation: Kalman, H_∞, and nonlinear approaches*. John Wiley & Sons, 2006.

[22] I. Marković, J. Ćesić, and I. Petrović, "On wrapping the Kalman filter and estimating with the SO(2) group," in *Int. Conf. Information Fusion*, July 2016, pp. 2245–2250.